

refrigerant pressure signal at the evaporator inlet. During all tests the evaporator will be flooded with HFC-134a (i.e., no superheating) by adjusting the opening of the metering valve mounted in series with the capillary tube.

The air temperature within the refrigerator will be controlled by PID driven electrical heaters, strategically placed in the freezer. The evaporator surface temperature will be measured by 10 T-type thermocouples, attached along the coil. The defrost heater temperatures will be monitored by K-type thermocouples. To accelerate the frost formation, water vapor will be released inside the fresh-food compartment by a PID-driven electrical heater immersed in a water reservoir.

In order to visualize the frost formation process and evaluate the defrost time, an insulating glass window of certain thickness will be the part of apparatus in the freezer rear wall. The defrost power will be monitored by a power transducer.

The different heater options and actuation modes were compared through a parameter known as the defrost efficiency. This parameter is defined as the ratio between the ideal energy, i.e., that required to melt the frost layer, and the energy that is actually released by the electrical heater, expressed as follows:

$$n_d = \frac{E_{id}}{E_r}$$

The ideal energy, E_{id} is composed of a sensible part, responsible for the temperature rise to 0°C, and a latent part, responsible for the phase change from solid to liquid. The real energy, E_r is the time integration of the power dissipated by the defrost system,

$$E_{id} = mc_{p,i}(T_{melt} - T_w) + mh_{sl}$$

$$E_r = \int_0^t W_d dt$$

where $c_{p,i}$ is the ice specific heat and T_{melt} and h_{sl} are, respectively, the water fusion temperature (0°C) and latent heat. The parameter T_w stands for the average temperature of the evaporator tubes, while m is the frost mass and W_d is the defrost power.

In addition to the defrost efficiency other parameters were analyzed, such as the average air temperature of the freezer compartment after defrost and the maximum temperature of the heater during defrost.

III. LITERATURE REVIEW

Christian J.L. Hermes et.al ^[1], The present study advances a theoretical and experimental investigation of the frost growth and densification on flat surfaces. This study focuses on the most important factors affecting the frost formation process, i.e. the surrounding air temperature, humidity and velocity, and the surface temperature. The processes of frost growth and densification were investigated experimentally in order to provide a physical basis for the development of a theoretical model to predict the variation of the frost layer thickness and mass with time. The mathematical model was based on mass and energy balances within the frost

Pradeep Bansal et.al ^[2], They have done a thermal analysis of a defrost cycle in order to design more efficient defrosting mechanisms in household refrigerators and freezers. A simple heat transfer model has been developed to determine energy flows from a defrost heater across various components of a refrigerator/freezer. The study measures power consumption and temperatures of a single temperature vertical empty freezer (in normal operation with and without defrosts) to determine the heat distribution from the radiant type electric defrost heater and its effect on power consumption. The surface temperature of the defrost heater was measured to be 520 °C for minimal frost and 560 °C for heavy frost. The efficiency of a defrost heater was measured to be 30.3%, while power consumption of the freezer was found to increase by 17.7% due to automatic defrost.

J. Alberto Dopazo et.al ^[3], Worked on a detailed transient simulation model has been developed to predict and evaluate the performance of the hot-gas defrost process of an air-coil evaporator. In the model, the defrost process is subdivided into six stages: preheating, tube frost melting start, fin frost melting start, air presence, tube-fin water film and dry-heating. In each stage, the control volume is subdivided into systems represented by a single node, which has the representative properties of the system. A finite difference approach was used to solve the model equations.

Christian J.L. Hermes et.al ^[4], Worked on an alternative test method to evaluate the energy consumption of frost-free refrigerators and freezers for residential applications. While the standardized methods require the refrigerating appliance to be kept running according to its onboard control system. These results were confirmed for a bottom-mount frost-free refrigerator with a forced-air condenser, with differences not exceeding 1%. However, in the case of the direct-cool refrigerator with natural draft condenser and evaporator was evaluated, the energy consumption discrepancy between the SSE and ISO test approaches was higher than 15%, which is speculated to be due to the limitations of applied to refrigerators that undergo longer transients.

Honghyun Cho et.al ^[5], This work present During the defrosting process, the temperature in the cabinet of a showcase becomes higher than the set point. This phenomenon is undesirable for foods or products stored Besides, the performance of each defrosting method was compared in terms of capacity, compressor power, COP, and storage temperature. As a result, the optimum EEV opening in this study was 75% of the full opening during the hot-gas bypass defrost. The hot-gas bypass defrosting cycle with sequential defrost of each evaporator showed advantages in achieving the appropriate refrigerating capacity and maintaining

constant storage temperature during the defrost even though it had a relatively higher compressor power compared to the on-off cycling.

IV.RESULTS

With different operating powers we found the defrost efficiencies of four different types of defrost heaters, keeping constant all the working conditions. The frost is shown in three stages in figure 1, 2, and 3 at 2h, 4h, and 8h respectively.

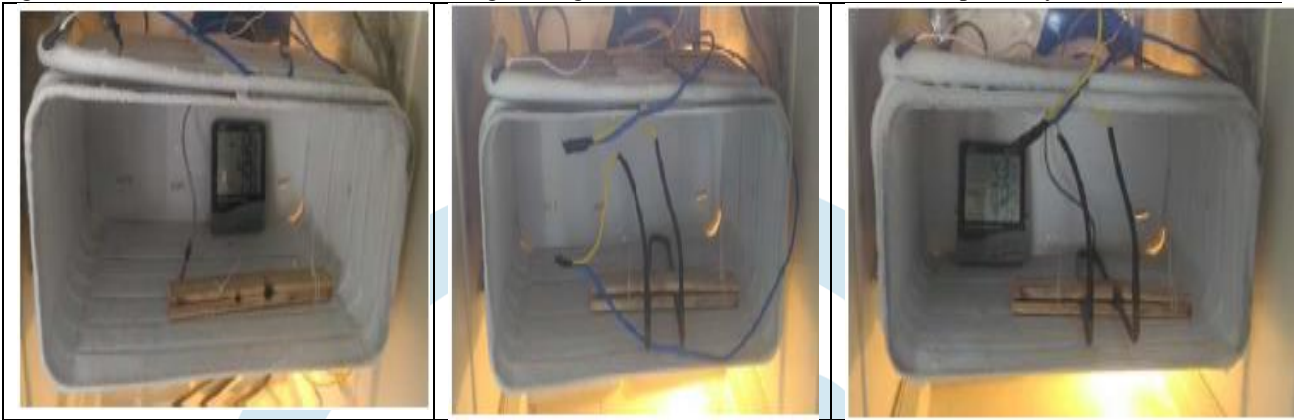


Fig 2 Freezer compartment

Table 1 Experiments result

Test	Heater	Mode	t[min]	W_d	T_h (°C)	T_w (°C)	m[g]	n_d [%]
1	U-type	Integral	24.8	110	275	23.9	155.2	27.32
2	U-type	Integral	19.6	160	327	22.1	155	24.02
3	U-type	Stepped	22.3	160 to 20	38	22.7	155.3	25.08
4	U-type	Pulsating	25	160 to 0	70.8	20	149	22.70
5	Distributed	Integral	19.8	160	237.3	23.1	147.3	21.70
6	Distributed	Stepped	21.2	160 to 20	40	4.3	157.1	29.88
7	Distributed	Pulsating	23	160 to 0	35.5	9.3	155.1	23.11
8	Glass tube	Integral	18.5	160	350	10	150	26.56
9	Glass tube	Stepped	20.1	160 to 20	330.5	2.2	159.3	32.37
10	Glass tube	Pulsating	20.9	160 to 0	332.5	3	158.9	28.21
11	Calrod	Integral	20.8	160	340	22.3	149.2	21.76
12	Calrod	Stepped	22.3	160 to 20	288.9	6.8	151.6	27.10
13	Calrod	Pulsating	22	160 to 0	278.6	6.1	150.9	23.77

In test 1 the u-type heater is run on integral power operating mode of this test was to calculate the time which is normally 9 to 11 min. in household refrigerator but with the experimental analysis with u-type heater 6 to 6.5 min. as visual from the fig.3 and the rest of the experiment is carried till the total frost is melted from the refrigerator temperature of evaporator is measured and plotted with respect to time during this respective test. The temperature T_0 and T_i indicator and the average of it T_w

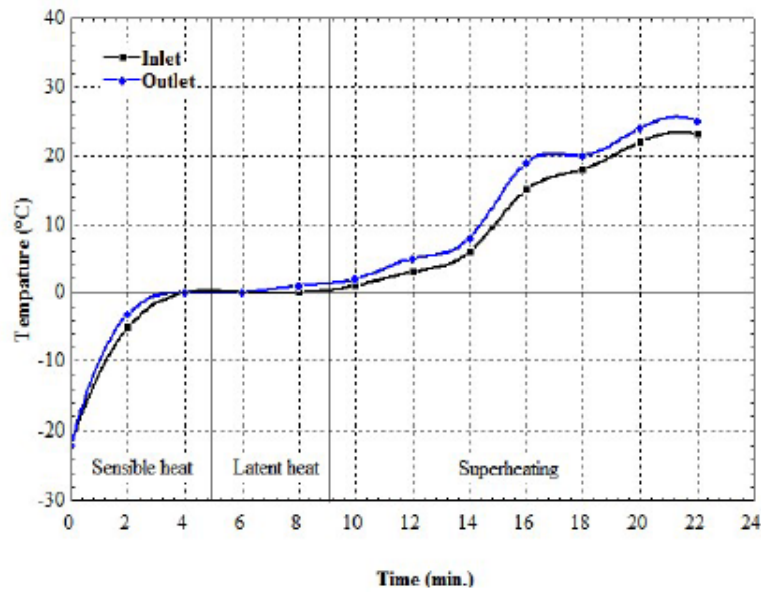


Fig 3

with 110 W, the purpose time taken by the defrost system to reach the 0°C temperature refrigerator compartment. The inlet and outlet are individually obtained from the multipoint temperature is obtained. Both the test one and two are carried with U type heater, and came to know that the defrost efficiency of the 1st than the 2nd as the power supplied to heater in 1st test is lower than the second test. Also while defrost the heater rises the freezer compartment temperature to 12°C, thus the load to compensate for the compressor increases the manufacturers, the defrost terminator, when placed at the where the evaporator takes long warmed, guarantees the complete elimination of the frost after the temperature exceeds 10°C.

The surface temperatures of distributed and U-type defrost heaters were not possible to read because of some experimental issues during the integral power. As shown in figure 4 the temperatures of glass tube and calrod are plotted with respect to time. Here we find that the glass tube temperature is higher than all other heaters during the integral power operating mode.

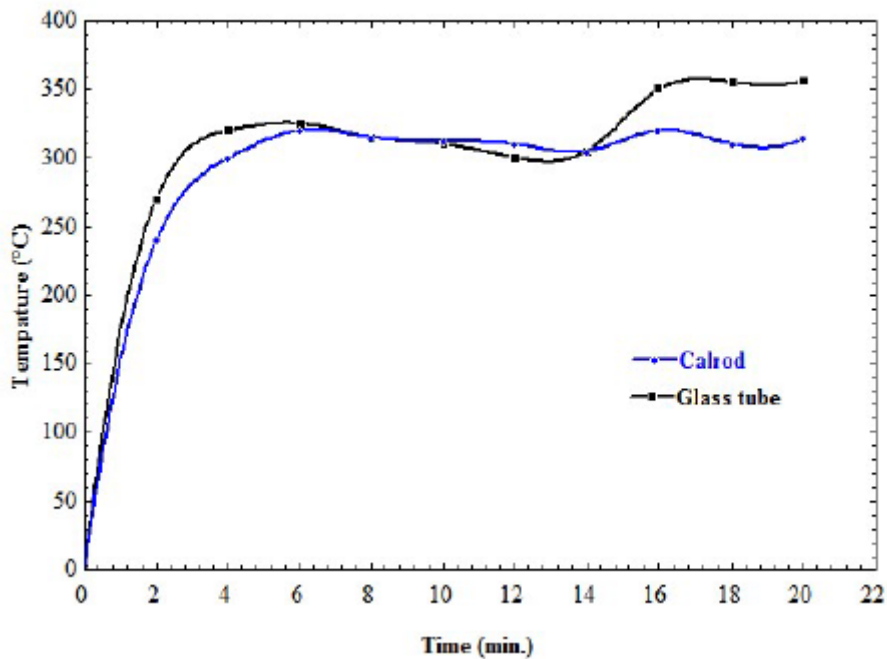


Fig 4

The efficiencies of tests at different operating modes are indicated in figure 5, here we found that the defrost efficiencies are almost identical but the defrost efficiencies of glass tube are highest among all the operating modes.

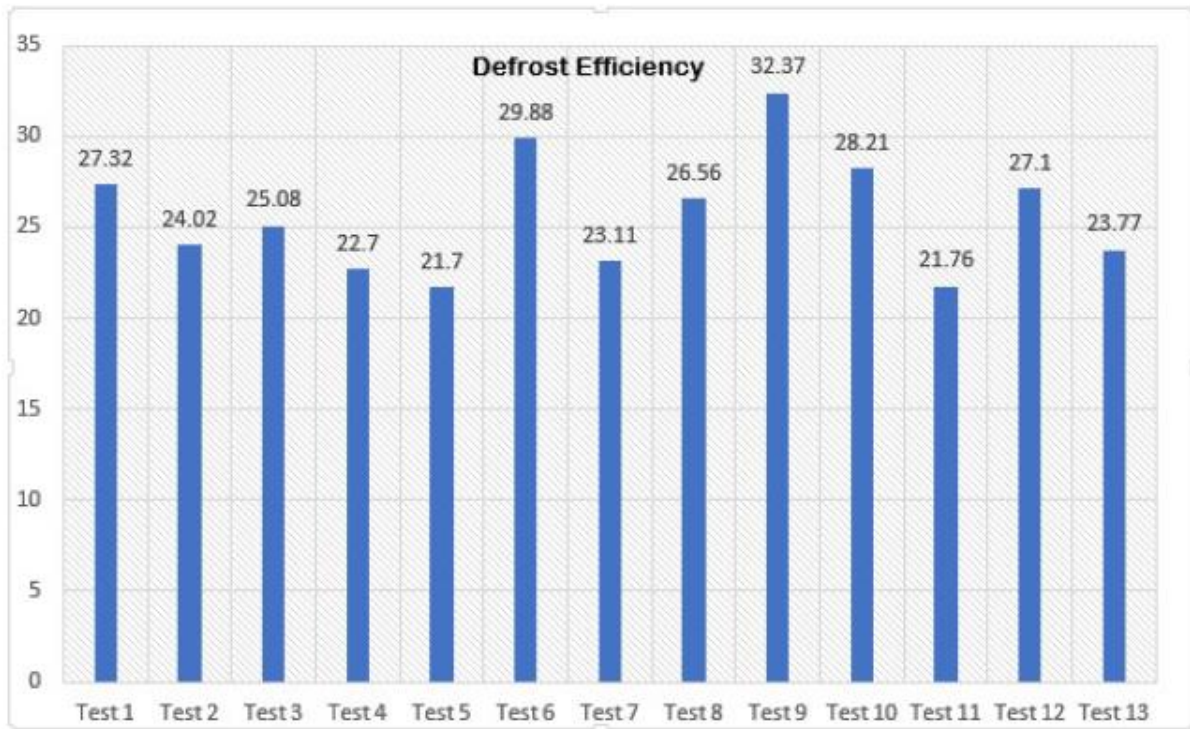


Fig 5

The purpose of tests 4, 7, 10 and 13 was to explore the effect of the pulsating operating mode, as illustrated in Fig. 6b. The length of each pulse was defined applying the same procedure used for the step length. It can be observed that the pulsating mode provides defrost efficiencies which are higher than the integral mode but lower than the steps mode.

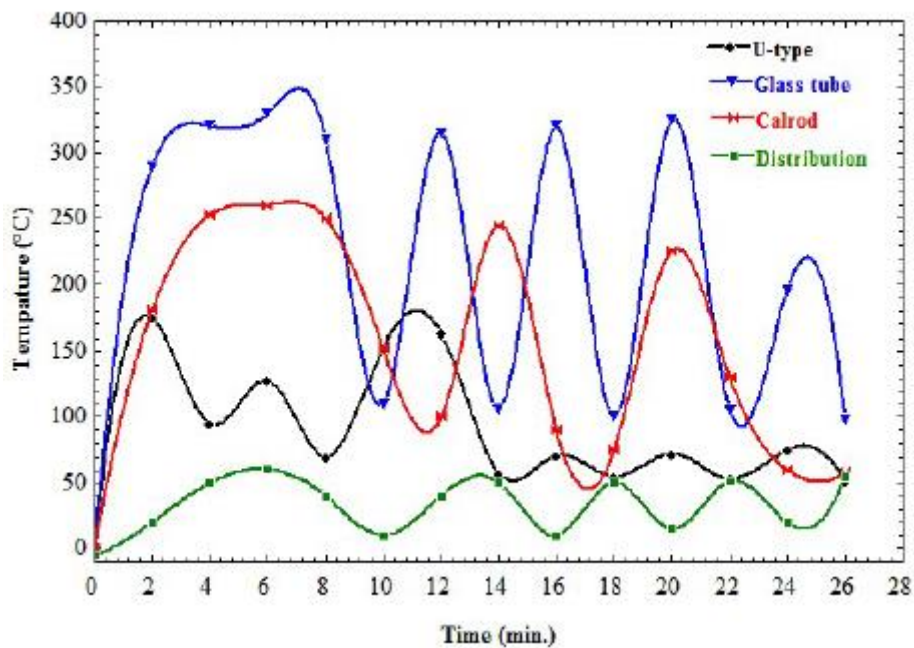


Fig 6(a) Heaters surface temp

It can also be seen that with the pulsating mode the defrost time with the distributed heater became lower than that obtained with the steps mode, which was reflected in the freezer air temperature.

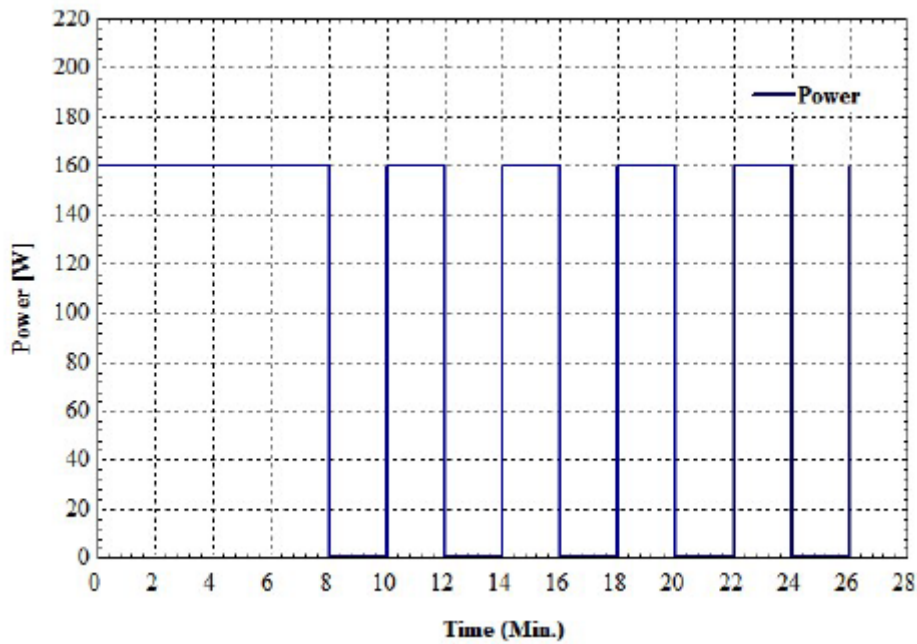


Fig 6(b) Heaters Power

Fig. 6a shows the heater temperatures during defrost. Once again it can be observed that the calrod and glass tube heaters reached considerably high temperatures during the initial transient period. However, during the cycling period the average temperature was substantially reduced, evidencing an advantage of this mode compared to the integral power mode.

As the defrost energy is a function of the accumulated frost mass, tests 3, 6, 9 and 12 were carried out. Defrost was conducted by gradually reducing the heater power in four 40 W steps, as illustrated in Fig. 6(b). The steps lengths were defined based on the tests with the step power operating mode. In this mode and with the U type heater (test 3) defrosts lasted 22.3 min and the average evaporator temperatures reached 22.7°C defrost.

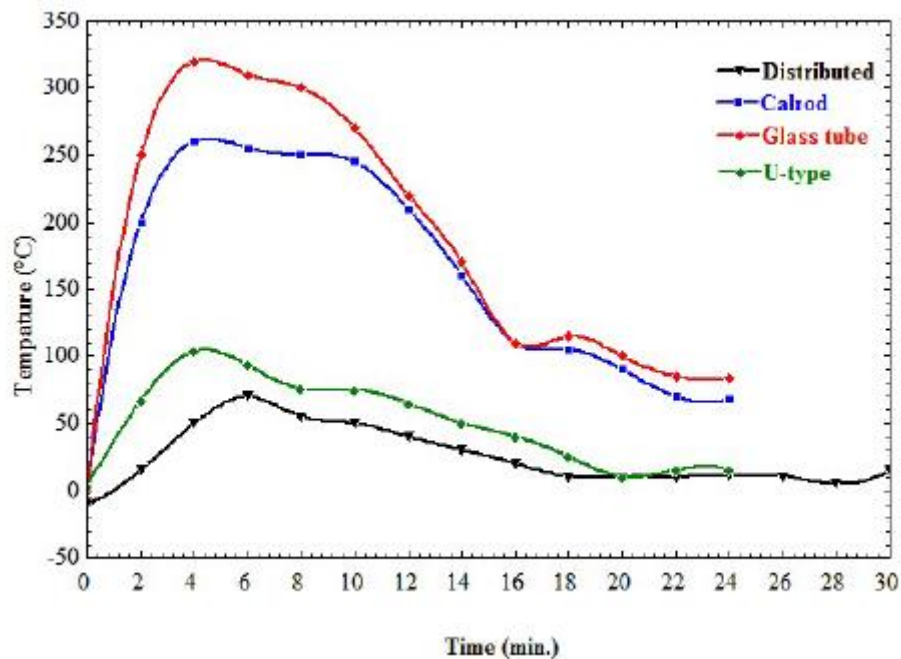


Fig 7(a) Heaters Surface temperatures

The first step length was then defined as 8 min, remaining further 14.3 min to conclude the defrosting. As the use of 40-W steps was selected 2 min steps were adopted. An analogous procedure was adopted for the calrod, distributed and glass tube heaters where step lengths of 4, 3 and 2 min were obtained, respectively.

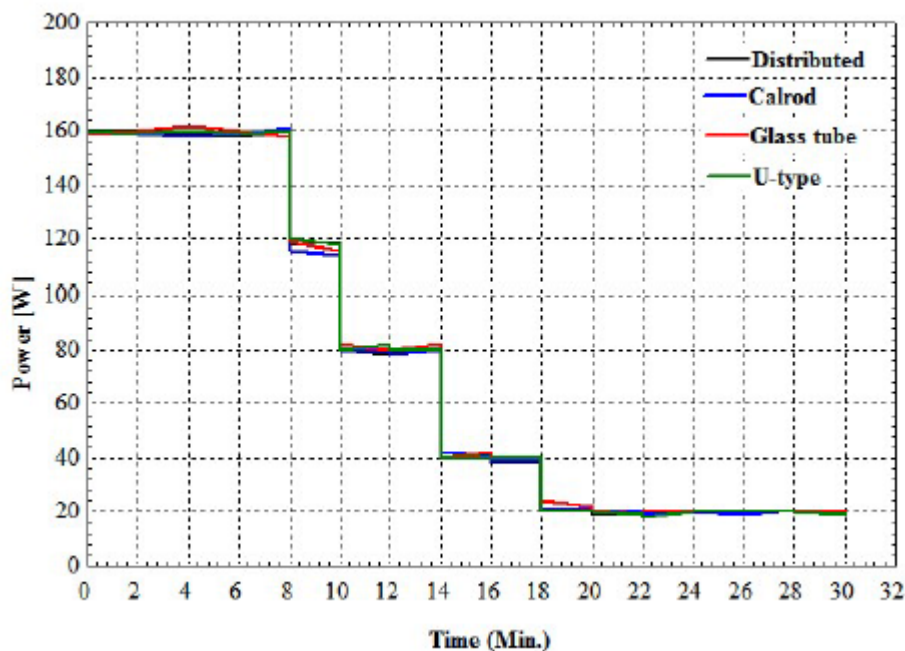


Fig 7(b) Heater Power

Unfortunately the adopted steps were not effective at completely eliminating the frost layer, which is evident considering the last step length. Nevertheless, as expected, the defrost efficiency increased in all cases. The defrost time, however, particularly for the distributed heater, increased in such way that it led to a considerable temperature rise within the freezer compartment after defrosting. Regardless of the result obtained with the steps operating mode, it is evident that through proper refinements substantial efficiency improvements can be achieved. It was also noted that the calrod and glass tube heaters once again reached high temperature levels, while the distributed heater remained below 80°C see fig 7(b). One of the advantage of step mode is that the heater temperature decreases with time, thus avoiding superheating of the parts surrounding the evaporator.

V. CONCLUSION

Considering the three operating modes investigated in this study, the power steps mode was found to be the most efficient, as illustrated in Fig.8 (a, b) (tests 3, 6, 9 and 12). In general it was concluded that all three types of heaters presented practically the same defrost efficiency in each operating mode. When operating in the steps mode, the glass tube heater provided the highest efficiency of approximately 32.37%, although the efficiency values obtained with the other heaters were very close. However, both defrost time and freezer air temperature after defrost were higher. The calrod and glass tube heaters did not warm the freezer as the distributed one did, but reached considerably higher temperatures, which could contribute to warming up the freezer when the compressor restarts. Considering that the defrost efficiency of the calrod heater is very close to the values obtained with the other types and that it is less expensive and easier to install, one can conclude that this type can be recommended for installation in a real application. It can also be concluded that it is possible to achieve significant improvements in the defrost efficiency by testing different combinations of time and power. It should be noted however that this analysis is limited, as previously stated. The gradual power reduction requires an operating time increase, which cannot be long, since the compressor should not remain off for extended periods. If this happens, the air temperature within the compartments rises and the compressor run time increases after defrost, thus increasing the energy consumption. Therefore, it is recommended that standardized energy consumption tests are carried out in order to identify the impact of the defrost efficiency on the refrigerator performance.

REFERENCES

- [1] HaijunJeong, et.al “Adaptive defrost methods for improving defrosting efficiency of household refrigerator”, *Energy Conversion and Management* 157 (2018) 511–516.
- [2] PradeepBansal*et.al “Thermal analysis of the defrost cycle in a domestic freezer”, *International journal of refrigeration* of 33(2010)589-599.
- [3] J. Alberto Dopazoet.al “Modelling and experimental validation of the hot-gas defrost process of an air-cooled evaporator”, *International journal of refrigeration* of 33(2010)829-839.
- [4] Christian J.L. Hermes et.al “Alternative test method to assess the energy performance of frost-free refrigerating appliances” *Applied Thermal Engineering* 121 (2017) 294–301.
- [5] SevgiUlutan.et.al “Dynamics of water vapor adsorption on humidity-indicating silicagel”, 9 August 2011, *International Communications in Heat and Mass Transfer* 38 (2011) 1384–1391.